Estimation of Wiener Phase Noise by the Autocorrelation of the ICI Weighting Function in OFDM Systems

Yi-Ching Liao and Kwang-Cheng Chen
Institute of Communication Engineering, College of Electrical Engineering
National Taiwan University, Taipei, Taiwan, 10617, R.O.C.
E-mail: ycliao@santos.ee.ntu.edu.tw, chenkc@cc.ee.ntu.edu.tw

Abstract— **Performance degradation due to Wiener phase noise which causes both common phase error (CPE) and inter-carrier interference (ICI) is a crucial challenge to the implementation of OFDM systems. In this paper, we theoretically employ the Lorentzian model to investigate the autocorrelation function of the ICI weighting function which is the discrete Fourier transform of the exponential phase noise process. This autocorrelation function can be shown to be the kernel of the covariance of the ICI. Based on this kernel, a pilot-aided decision-directed CPE estimator is proposed according to maximum-likelihood criterion. Different from conventional maximum likelihood approach which ideally assumes the ICI observed on different subcarriers to be independent identically distributed, we systematically derive the covariances among carriers and practically utilize them to enhance the estimation. Finally, three conventional CPE estimators are compared with the proposed scheme by computer simulation, the numerical results illustrate the effectiveness of the proposed algorithm.**

Index Terms— **OFDM, Phase Noise and Maximum Likelihood Estimation.**

I. Introduction

Orthogonal frequency division multiplexing (OFDM) has been attracting considerable research interests as a promising candidate to high data rate communications since its resistance to impairments such as frequency selective fading and impulsive noise. However, OFDM is tremendously more sensitive to carrier frequency offset and phase noise than single carrier systems [1]. Mainly resulting from the instability of local oscillator, phase noise can be classified into two categories. When the system is only frequency-locked, the resulting phase noise is modeled as a zero-mean Wiener process. When the system is phase-locked, the resulting phase noise is modeled as a zero-mean stationary random process [2]. Here, we concentrate on the suppression of Wiener phase noise.

Methods for the compensation of the effects of phase noise have been proposed by several authors. The conventional approaches can be categorized into decision directed approaches and pilot-aided approaches. The decision directed approaches [3], [4], estimate the CPE using the averaged phase rotation of the observed symbols from the ideal constellation points. A symbol by symbol pre-compensation is necessary to ensure this rotation not exceeding the decision boundary. As for pilot-aided approach [5]–[7], the average or weighted average of the phase differences between the transmitted and received pilot symbols are used to estimate the CPE.

In this paper, by using the Lorentzian model, the autocorrelation function of the ICI weighting function which can be shown to be the kernel of the second order statistics of the ICI is systematically derived. Different from conventional maximum likelihood (ML) schemes [4], [7] which ideally assume the ICI observed on different subcarriers to be independent identically distributed, we practically investigate their covariances by the autocorrelation function of the ICI weighting function and combine pilot-aided and decision-directed approaches to yield a generalized maximum likelihood estimation scheme. Simulation results demonstrate that the proposed algorithm outperforms the conventional approaches

The rest of this paper is organized as follows: Section II presents the phase noise corrupted OFDM signal model and the phase noise model respectively. Based on that, Section III first investigate the statistical characteristics of the sufficient statistics, then, it proceed to derive the maximum likelihood estimator for the CPE. Performance evaluation via computer simulation is addressed in Section IV. Finally, Section V discusses and concludes this paper.

II. Background

A. Phase Noise Corrupted OFDM Signal Model

Considering a general OFDM system using N-point inverse fast Fourier transform (IFFT) for modulation. Assume the frequency domain subcarrier index set is composed of three mutually exclusive subsets defined by

$$\begin{aligned}\mathcal{D} &\triangleq \{d_1, d_2, \cdots, d_{N_d}\}\\ \mathcal{P} &\triangleq \{p_1, p_2, \cdots, p_{N_p}\}\\ \mathcal{N} &\triangleq \{n_1, n_2, \cdots, n_{N_n}\},\end{aligned} \tag{1}$$

where $\mathcal{D}$ denotes the set of indices for N_d data-conveying subcarriers, $\mathcal{P}$ is the set of indices for N_p pilot subcarriers and $\mathcal{N}$ stands for N_n virtual subcarriers. Then, the set of indices for N_u useful subcarriers $\mathcal{U}$ can be defined as

$$\mathcal{U} \triangleq \{u_1, u_2, \cdots, u_{N_u}\} = \mathcal{D} \cup \mathcal{P}, \tag{2}$$

where $N_u = (N_d + N_p)$. Let $X_m(k)$ be the modulated symbol on the kth subcarrier of the mth OFDM symbol. For $k \in \mathcal{U}$,

978-3-8007-2909-8/05/$20.00 ©2005 IEEE

$X_m(k)$ is taken from some constellation with zero mean and average power $\sigma_X^2 \equiv E\{|X_m(k)|^2\}$. The output of the IFFT has a duration of T seconds which is equivalent to N samples. A N_g-sample cyclic prefix longer than the channel impulse response is preceded to eliminate the inter-symbol interference (ISI).

At the receiver, timing and frequency recovery is assumed to be accomplished. Considering the multiplicative phase noise and the additive white noise, the received nth sample of the mth OFDM symbol can be written as

$$r_m(n) = [x_m(n) \otimes h_m(n)]\, e^{j(\phi_m(n)+\theta)} + \xi_m(n) \tag{3}$$

in which $\otimes$ is the circular convolution and

$$\phi_m(n) = \phi\left(m(N+N_g) + N_g + n\right) \tag{4}$$

where $x_m(n)$, $h_m(n)$ and $\phi_m(n)$ represent the transmitted signal, the channel impulse response and the phase noise respectively, while $\xi_m(n)$ denotes the AWGN noise and θ is the initial phase of the phase noise process. After removing the cyclic prefix and performing the FFT, the frequency domain symbol can be expressed by

$$\begin{aligned} R_m(k) =& \Phi_m(0)H_m(k)X_m(k) \\ &+ \underbrace{\sum_{\substack{l\in\mathcal{U} \\ l\neq k}} \Phi_m(k-l)H_m(l)X_m(l)}_{I_m(k)} + Z_m(k) \end{aligned} \tag{5}$$

where $H_m(k)$ is the channel frequency response and $Z_m(k)$ denotes the frequency domain expression of $\xi_m(n)$. $\Phi_m(h)$ is the discrete Fourier transform of the phase noise process given by

$$\Phi_m(h) = \frac{1}{N}\sum_{n=0}^{N-1} e^{j(\phi_m(n)+\theta)} e^{-j2\pi\frac{hn}{N}}. \tag{6}$$

And it can be viewed as a weighting function on the transmitted frequency domain symbols. In particular, when $h = 0$, $\Phi_m(0)$ is the time average of the phase noise process within one OFDM symbol duration. This term is usually known as the common phase error (CPE) which causes the same phase rotation and amplitude distortion to each transmitted frequency domain symbol. On the other hand, when $h \neq 0$, the second term in (5) is the inter-carrier interference (ICI) resulting from the contributions of other subcarriers by the weighting of $\Phi_m(h)$ due to the loss of orthogonality. In the rest of this paper, we shall call $\Phi_m(h)$ the ICI weighting function.

Based on (5), the received frequency domain vector can be given by

$$\begin{aligned} \boldsymbol{r}_m &= \Phi_m(0)\boldsymbol{H}_m\boldsymbol{x}_m + \boldsymbol{\iota}_m + \boldsymbol{\zeta}_m \\ &= \Phi_m(0)\boldsymbol{H}_m\boldsymbol{x}_m + \boldsymbol{\varepsilon}_m, \end{aligned} \tag{7}$$

where $\boldsymbol{\varepsilon}_m = \boldsymbol{\iota}_m + \boldsymbol{\zeta}_m$,

$$\begin{aligned} \boldsymbol{H}_m &\triangleq diag(H_m(0), H_m(1), \cdots, H_m(N-1)) \\ \boldsymbol{x}_m &\triangleq \left[X_m(0) \quad X_m(1) \quad \cdots \quad X_m(N-1)\right]^T \\ \boldsymbol{\iota}_m &\triangleq \left[I_m(0) \quad I_m(1) \quad \cdots \quad I_m(N-1)\right]^T \\ \boldsymbol{\zeta}_m &\triangleq \left[\zeta_m(0) \quad \zeta_m(1) \quad \cdots \quad \zeta_m(N-1)\right]^T, \end{aligned} \tag{8}$$

and $diag(\cdot)$ is a diagonal matrix. From now on, we shall add a second subscript to one of the vector or matrix variables defined in (7) and (8) to indicate its sub-vector or sub-matrix which is taken according to one of the subcarrier index sets in (1) and (2). The second subscript may be chosen from $\{p, d, n, u\}$ which relates to $\{\mathcal{P}, \mathcal{D}, \mathcal{N}, \mathcal{U}\}$ respectively. For example,

$$\boldsymbol{r}_{m,p} = \left[R_m(p_1) \quad R_m(p_2) \quad \cdots \quad R_m(p_{N_p})\right]^T \tag{9}$$

stands for the received pilot vector.

Conventionally, $\boldsymbol{r}_{m,p}$ is utilized to obtain the channel response and common phase error to carry out equalization on $\boldsymbol{r}_{m,d}$, then the equalized results are sent to the detection block to get the decisions. Since accurate channel estimation in OFDM systems can be obtained by either preambles or pilot symbols [8], in the following sections we assume that the channel frequency response is acquired perfectly at the receiver.

B. Phase Noise Model

Accurate modeling of oscillator phase noise is a key factor to the analysis and simulation of the distortion caused by phase noise. For a classic model of phase noise, $\phi_m(n)$ can be modeled as a discrete-time Wiener process [1] with

$$\begin{aligned} &E[\phi_m(n)] = 0 \\ &E[(\phi_m(n+\Delta n) - \phi_m(n))^2] = 4\pi\beta T|\Delta n|/N, \end{aligned} \tag{10}$$

where β (Hz) denotes the one-sided 3 dB linewidth of the Lorentzian power density spectrum of the free-running oscillator. The Lorentzian spectrum is the squared magnitude of a first order lowpass filter transfer function [8]. The single-sided spectrum $S_\Phi(f)$ is given by

$$S_\Phi(f) = \frac{2/\pi\beta}{1+f^2/\beta^2}, \tag{11}$$

and the Lorentzian spectra with different one-sided 3 dB linewidth are shown in Figure 1.

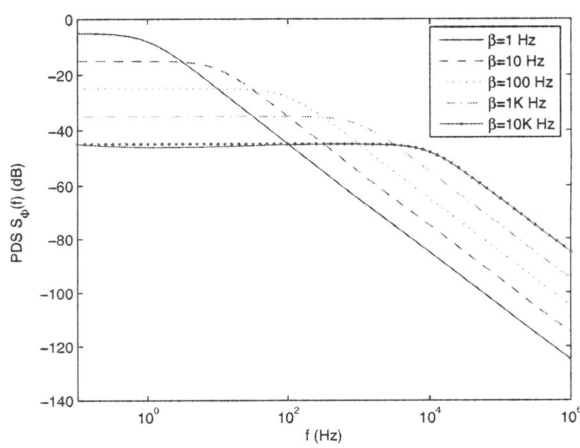

Fig. 1. Lorentzian spectrum with different one-sided 3 dB linewidth

As for the initial phase θ, it can be modeled as a random variable uniformly distributed in $[0, 2\pi)$ and is independent of $\phi_m(n)$. Later analysis and simulation will be based on this model.

III. Pilot-Aided Decision-Directed CPE Estimation

Most OFDM systems employ pilots to facilitate receiver synchronization since data-aided estimation gives better and steadier estimate. However, since pilots cost system utilization, the number of pilots should be kept as low as possible which confines the performance of pilot-aided CPE estimation algorithms. Comparatively, decision-directed approaches enjoy a larger observation space. Nevertheless, ensuring the acceptable correctness of the decisions is also critical. Therefore, use pilots to acquire the CPE and provide an initial compensation, then enlarge the observation space by including the tentative decisions as the sufficient statistics to perform the final estimate can benefit from the advantages of both approaches. We refer this method to the pilot-aided-decision-directed (PADD) approach. In the following, we shall investigate the statistical characteristics of the sufficient statistics $\boldsymbol{r}_{m,u}$ and systematically derive the ML estimator in accordance with the PADD approach.

A. Statistical Characteristics of the Sufficient Statistics

Considering the PADD approach, since the data and the channel frequency response are acquired, the statistical characteristics of $\boldsymbol{r}_{m,u}$ depend on that of $\boldsymbol{\iota}_{m,u}$ and $\boldsymbol{\zeta}_{m,u}$. The AWGN noise on each subcarrier can be modeled as a zero mean complex Gaussian random variable with variance σ_Z^2. Since the ICI on each subcarrier is composed of the data symbols on other subcarriers, we can apply the central limit theorem to model it as a complex Gaussian random variable. In the following, we first show that the ICI has a zero mean, then, the second order statistics of the ICI will be investigated.

1) The Mean of the ICI: Since $X_m(k)$ and $H_m(k)$ are assumed to be known in the PADD circumstance, the mean of the ICI depends on that of the ICI weighting function $\Phi_m(h)$ which can be expressed as

$$E[\Phi_m(h)] = \frac{1}{N}\sum_{n=0}^{N-1} E\left[e^{j(\phi_m(n)+\theta)}\right] e^{j2\pi\frac{hn}{N}}. \tag{12}$$

Since θ is independent of $\phi_m(n)$, the expectation in (12) can be decomposed into the product of $E[e^{j\phi_m(n)}]$ and $E[e^{j\theta}]$. Let $\Psi_\theta(\omega)$ denotes the characteristic function of the uniform random variable, we have

$$\begin{aligned} E[e^{j\theta}] &= \Psi_\theta(\omega)\big|_{\omega=1} \\ &= \frac{2}{2\pi\omega}\sin\left(\frac{2\pi\omega}{2}\right)e^{j\pi\omega}\Big|_{\omega=1} \\ &= 0. \end{aligned} \tag{13}$$

Therefore, the mean of the ICI becomes zero.

2) The Second Order Statistics of the ICI: In the PADD scenario, the sufficient statistics are the received useful symbols given by

$$\boldsymbol{r}_{m,u} = \Phi_m(0)\boldsymbol{H}_{m,u}\boldsymbol{x}_{m,u} + \boldsymbol{\iota}_{m,u} + \boldsymbol{\zeta}_{m,u}. \tag{14}$$

We may denote the covariance matrix of $\boldsymbol{\iota}_{m,u}$ by $\boldsymbol{C}_{\boldsymbol{\iota}_{m,u}}$, then the covariance matrix of $\boldsymbol{r}_{m,u}$ can be expressed as

$$\boldsymbol{C}_{\boldsymbol{r}_{m,u}} = \boldsymbol{C}_{\boldsymbol{\iota}_{m,u}} + \sigma_Z^2\boldsymbol{I}. \tag{15}$$

Let the element of $\boldsymbol{C}_{\boldsymbol{\iota}_{m,u}}$ be denoted by $\sigma_i(k1, k2)$, it can be expressed as

$$\begin{aligned} \sigma_i(k_1,k_2) = &\sum_{\substack{l_1\in\mathcal{U}\\ l_1\neq u_{k_1}}}\sum_{\substack{l_2\in\mathcal{U}\\ l_2\neq u_{k_2}}} H_m(l_1)H_m^*(l_2)X_m(l_1)X_m^*(l_2) \\ &E\left[\Phi_m(u_{k_1}-l_1)\Phi_m^*(u_{k_2}-l_2)\right]. \end{aligned} \tag{16}$$

We can observe that $\sigma_i(k1, k2)$ depends on the autocorrelation function of the ICI weighting function $\Phi_m(h)$. Therefore, we have the following proposition.

Proposition 1 (The autocorrelation function of $\Phi_m(h)$): For a Wiener phase noise with the Lorentzian spectrum, given the one-sided 3 dB linewidth β, the autocorrelation function of the ICI weighting function $\Phi_m(h)$ can be defined by $R_\Phi(h1, h2) \equiv E[\Phi_m(h_1)\Phi_m^*(h_2)]$ and

$$\begin{aligned} R_\Phi(h1,h2) = &\frac{\delta_{(h_1-h_2)_N}}{N^2}\left[N + \frac{1-N+Ne^{z_1}-e^{Nu}}{2-e^{z_1}-e^{-z_1}}\right. \\ &\left.+\frac{1-N+Ne^{\bar{z}_2}-e^{Nu}}{2-e^{\bar{z}_2}-e^{-\bar{z}_2}}\right] \\ &+\frac{(1-\delta_{(h_1-h_2)_N})}{N^2}\frac{1-e^{Nu}}{1-e^{(z_1-z_2)}} \\ &\left(\frac{1}{1-e^{z_1}}-\frac{1}{1-e^{\bar{z}_1}}+\frac{1}{1-e^{\bar{z}_2}}-\frac{1}{1-e^{z_2}}\right) \end{aligned} \tag{17}$$

where

$$\begin{aligned} z_1 &\equiv u + jv_1 \equiv -\frac{2\pi}{N}\left[\beta T + jh_1\right] \\ z_2 &\equiv u + jv_2 \equiv -\frac{2\pi}{N}\left[\beta T + jh_2\right] \end{aligned} \tag{18}$$

and $(\cdot)_N$ denotes the modulo by N, $\bar{z}$ represents the complex conjugate of z.

Proof: cf. Appendix. ■

As for σ_Z^2, since it can be obtained by preamble signal and has been proposed in the literature [9], we may assume that σ_Z^2 is known by the receiver henceforth.

B. Maximum Likelihood CPE Estimator

From the above discussion, the sufficient statistics $\boldsymbol{r}_{m,u}$ can be modeled as a complex Gaussian random vector with mean vector $\Phi_m(0)\boldsymbol{H}_{m,u}\boldsymbol{x}_{m,u}$ and covariance matrix $\boldsymbol{C}_{\boldsymbol{r}_{m,u}}$. Hence, the log-likelihood function shall be

$$\begin{aligned} \Lambda\left(\Phi_m(0)\right) = &2\Re\left\{\boldsymbol{x}_{m,u}^H\boldsymbol{H}_{m,u}^H\boldsymbol{C}_{\boldsymbol{r}_{m,u}}^{-1}\boldsymbol{r}_{m,u}\Phi_m^*(0)\right\} \\ &-\boldsymbol{x}_{m,u}^H\boldsymbol{H}_{m,u}^H\boldsymbol{C}_{\boldsymbol{r}_{m,u}}^{-1}\boldsymbol{H}_{m,u}\boldsymbol{x}_{m,u}|\Phi_m(0)|^2. \end{aligned} \tag{19}$$

To find the ML estimation of $\Phi_m(0)$, we may first let $\Phi_m(0) = A_m e^{j\phi_m}$ and let the derivatives of (19) w.r.t. A_m and ϕ_m equal to zero to get

$$\begin{cases} \hat{\phi}_m = \measuredangle \left\{ \boldsymbol{x}_{m,u}^H \boldsymbol{H}_{m,u}^H \boldsymbol{C}_{\boldsymbol{r}_{m,u}}^{-1} \boldsymbol{r}_{m,u} \right\} \\ \hat{A}_m = \dfrac{\boldsymbol{x}_{m,u}^H \boldsymbol{H}_{m,u}^H \boldsymbol{C}_{\boldsymbol{r}_{m,u}}^{-1} \boldsymbol{r}_{m,u} e^{-j\hat{\phi}_m}}{\boldsymbol{x}_{m,u}^H \boldsymbol{H}_{m,u}^H \boldsymbol{C}_{\boldsymbol{r}_{m,u}}^{-1} \boldsymbol{H}_{m,u} \boldsymbol{x}_{m,u}}. \end{cases} \tag{20}$$

Then, the ML estimation of the CPE will be

$$\hat{\Phi}_m(0) = \frac{\boldsymbol{x}_{m,u}^H \boldsymbol{H}_{m,u}^H \boldsymbol{C}_{\boldsymbol{r}_{m,u}}^{-1} \boldsymbol{r}_{m,u}}{\boldsymbol{x}_{m,u}^H \boldsymbol{H}_{m,u}^H \boldsymbol{C}_{\boldsymbol{r}_{m,u}}^{-1} \boldsymbol{H}_{m,u} \boldsymbol{x}_{m,u}}. \tag{21}$$

IV. Performance Simulation

The proposed maximum-likelihood CPE estimator are evaluated in frequency selective slowly fading channels with 50 ns and 75 ns rms delay spread [10]. Channel impulse response remains static within a frame containing 16 symbols, but varies independently from frame to frame. Transmitted data is constructed according to the IEEE 802.11a standard [11]. 16 QAM and 64 QAM which are more sensitive to phase noise than M-PSK, are used in the simulation. The phase noise is simulated using the Lorentzian model with β equals to 1 kHz and 2 kHz. Pilot-aided approaches based on averaged-phase [5], weighted-averaged-phase [6] and least-square criterion [7] are also simulated as a comparison. Each simulation point is conducted by $3 \cdot 10^5$ OFDM symbols. The probability of symbol error (SER) with 16 QAM and 64 QAM in different channels are shown in Figure 2 and Figure 3 respectively.

It is easy to observe that Wiener phase noise causes an irreducible error floor to OFDM receiver performance, which is unacceptable in practice. About the effect of different channels, comparing Fig. 2(a) with Fig. 2(b), we can find that the shorter rms delay spread gives the better performance which is also evident in Fig 3. Observing Fig. 2 which corresponds to 16 QAM modulation, in general, the proposed ML estimator and the LS estimator greatly outperform the averaged-phase and weighted-averaged-phase approach. The performance gaps between the proposed ML estimator and the LS estimator at moderate SNR are 1 dB under 1 kHz linewidth and 2 dB under 2 kHz linewidth respectively.

In Fig. 3 which corresponds to 64 QAM modulation, we can observe that the performance of the three conventional approaches get closer and the performance gap between the two average based approaches and the proposed ML estimator become smaller compared to 16 QAM. And the performance gaps between the proposed ML estimator and the LS estimator at moderate SNR are 2.5 dB under 1 kHz linewidth and 2 dB under 2 kHz linewidth respectively. This phenomenon is mainly caused by the shrink of the decision boundary when employing high order modulation.

V. Conclusions

In this paper, a CPE estimator to effectively remove the complex gain caused by Wiener phase noise on the frequency domain transmitted symbols is proposed. We systematically derive the autocorrelation function of the ICI weighting function based on the Lorentzian model. The second order statistics of the ICI can be obtained by this autocorrelation function. Different from the conventional ML approaches which do not consider the statistic of Wiener phase noise, we investigate the covariances between the ICI observed on different subcarriers to yield a generalized maximum likelihood estimator. The effectiveness of the proposed algorithm is manifested by simulations and is shown to outperform the conventional schemes.

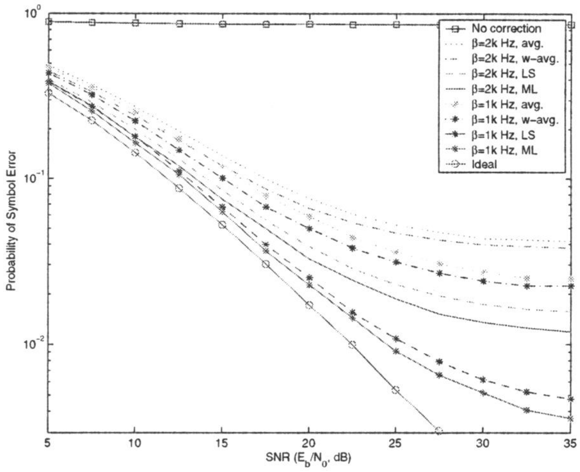

(a) rms delay spread = 50 ns

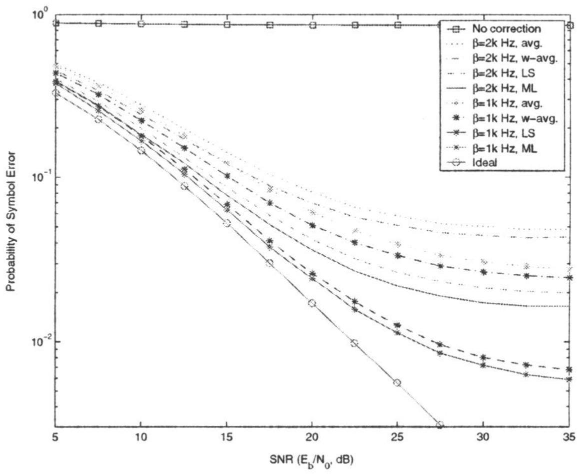

(b) rms delay spread = 75 ns

Fig. 2. SER Performance of the CPE correction schemes with 16 QAM

Appendix
Proof of Proposition 1

By definition, considering (6), the autocorrelation function of $\Phi(h)$ can be expressed as

$$\sum_{n_1=0}^{N-1} \sum_{n_2=0}^{N-1} \frac{E\left[e^{j(\phi_m(n_1)-\phi_m(n_2))}\right]}{N^2} e^{j2\pi \frac{h_2 n_2 - h_1 n_1}{N}}. \tag{22}$$

By (10), $\phi_m(n_1) - \phi_m(n_2)$ can be treated as a Gaussian random variable with zero mean and variance $4\pi\beta T|n_1 - n_2|/N$. Therefore,

$$E\left[e^{j(\phi_m(n_1)-\phi_m(n_2))}\right] = e^{-2\pi\beta T \frac{|n_1 - n_2|}{N}}. \tag{23}$$

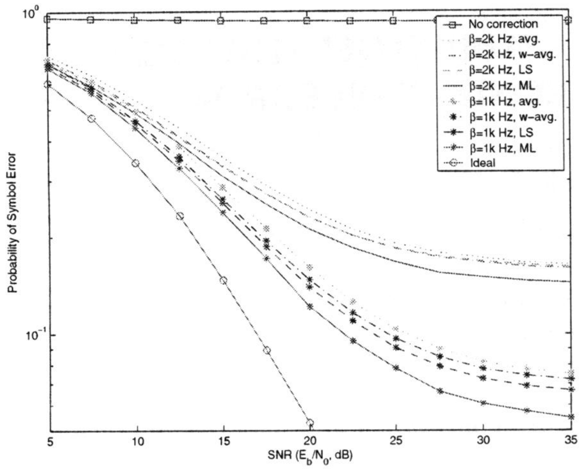

(a) rms delay spread = 50 ns

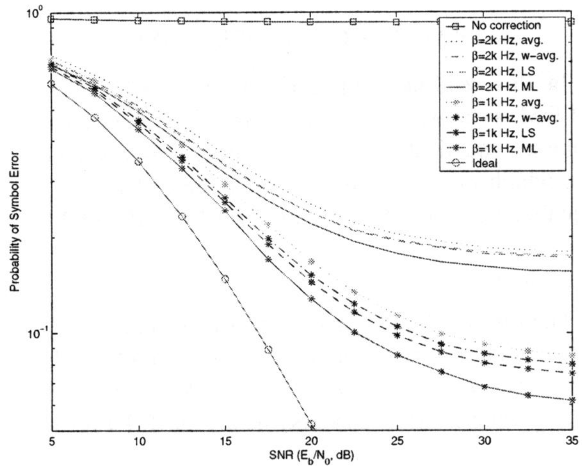

(b) rms delay spread = 75 ns

Fig. 3. SER Performance of the CPE correction schemes with 64 QAM

Substitute (23) into (22), we have

$$R_\Phi(h_1,h_2)=\sum_{n_1=0}^{N-1}\sum_{n_2=0}^{N-1}\frac{e^{-2\pi\beta T\frac{|n_1-n_2|}{N}}e^{j2\pi\frac{h_2n_2-h_1n_1}{N}}}{N^2}. \quad (24)$$

Let $N^2R_\Phi(h_1,h_2)$ be denoted by S_1, then divide the double summation into two parts as follows

$$S_1=\sum_{n=0}^{N-1}e^{j2\pi\frac{(h_2-h_1)n}{N}}+\sum_{n_1=1}^{N-1}\sum_{n_2=0}^{n_1-1}e^{-2\pi\beta T\frac{(n_1-n_2)}{N}} \left(e^{j2\pi\frac{h_2n_2-h_1n_1}{N}}+e^{j2\pi\frac{h_2n_1-h_1n_2}{N}}\right). \quad (25)$$

It is easy to show that the first summation in (25) is $N\delta_{(h_1-h_2)_N}$. Let the double summation in (25) be denoted by S_2 and use change of variable by letting $t=n_1-n_2$, we have

$$S_2=\sum_{t=1}^{N-1}\sum_{n_2=0}^{N-1-t}e^{j2\pi\frac{(h_2-h_1)n_2}{N}}\left(e^{-j2\pi\frac{h_1t}{N}}+e^{j2\pi\frac{h_2t}{N}}\right)e^{\frac{-2\pi\beta Tt}{N}}. \quad (26)$$

Carry out the summation of n_2, it becomes

$$\begin{aligned}S_2=&\delta_{(h_1-h_2)_N}\left[\sum_{t=1}^{N-1}(N-t)\left(e^{-j2\pi\frac{h_1t}{N}}+e^{j2\pi\frac{h_2t}{N}}\right)e^{\frac{-2\pi\beta Tt}{N}}\right]\\&+\frac{\left(1-\delta_{(h_1-h_2)_N}\right)}{1-e^{j2\pi\frac{h_2-h_1}{N}}}\sum_{t=1}^{N-1}\left(e^{-j2\pi\frac{h_1t}{N}}-e^{j2\pi\frac{h_1t}{N}}\right.\\&\left.+e^{j2\pi\frac{h_2t}{N}}-e^{-j2\pi\frac{h_2t}{N}}\right)e^{\frac{-2\pi\beta Tt}{N}}.\end{aligned} \quad (27)$$

In (27), we may denote the first and the second summation by Q_1 and Q_2 respectively. Since They are composed of geometric series, by the definition in (18), after some manipulation,

$$Q_1=\frac{1-N+Ne^{z_1}-e^{Nu}}{2-e^{z_1}-e^{-z_1}}+\frac{1-N+Ne^{\bar{z}_2}-e^{Nu}}{2-e^{\bar{z}_2}-e^{-\bar{z}_2}}, \quad (28)$$

and

$$Q_2=(1-Nu)\left(\frac{1}{1-e^{z_1}}-\frac{1}{1-e^{\bar{z}_1}}+\frac{1}{1-e^{\bar{z}_2}}-\frac{1}{1-e^{z_2}}\right). \quad (29)$$

Finally, $R_\Phi(h_1,h_2)$ can be iteratively evaluated and given by

$$\begin{aligned}R_\Phi(h_1,h_2)&=\frac{S_1}{N^2}=\frac{N\delta_{(h_1-h_2)_N}+S_2}{N^2}\\&=\frac{\delta_{(h_1-h_2)_N}(N+Q_1)}{N^2}+\frac{(1-\delta_{(h_1-h_2)_N})Q_2}{N^2(1-e^{z_1-z_2})}.\end{aligned} \quad (30)$$

Q.E.D.

REFERENCES

[1] T. Pollet, M. Van Bladel, and M. Moeneclaey, "BER sensitivity of OFDM systems to carrier frequency offset and wiener phase noise," *IEEE Trans. Commun.*, vol. 43, pp. 191–193, Feb./March/April 1995.

[2] L. Piazzo and P. Mandarini, "Analysis of phase noise effects in ofdm modems," *IEEE Trans. on Comm.*, vol. 50, no. 10, pp. 1696–1705, Oct 2002.

[3] V. Abhayawardhana and I. Wassell, "Common phase error correction for OFDM in wireless communication," in *Proc. IEEE Global Telecommun. Conf. (Globecom'02)*, vol. 1, Taipei, ROC, Nov. 2002, pp. 17–21.

[4] K. Nikitopoulos and A. Polydoros, "Compensation schemes for phase noise and residual frequency offset in OFDM systems," in *Proc. IEEE Global Telecommun. Conf. (Globecom'01)*, vol. 1, San Antonio, TX, Nov. 2001, pp. 25–29.

[5] T. Onizawa, M. Mizoguchi, T. Sakata, and M. Morikura, "A new simple adaptive phase tracking scheme employing phase noise estimation for OFDM signals," in *Proc. IEEE VTC'02 Spring*, vol. 3, Birmingham, AL, May 2002, pp. 1252–1256.

[6] P. Robertson and S. Kaiser, "Analysis of the effects of phase-noise in orthogonal frequency division multiplex (OFDM) systems," in *Proc. IEEE Int. Conf. Commun. (ICC'95)*, vol. 3, Seattle, WA, June 1995, pp. 1652–1657.

[7] S. Wu and Y. Bar-Ness, "A phase noise suppression algorithm for OFDM-based WLANs," *IEEE Commun. Lett.*, vol. 6, pp. 535–537, Dec. 2002.

[8] R. Van Nee and R. Prasad, *OFDM for Multimedia Wireless Communications*. Boston, MA: Artech House, 2000.

[9] S. He and M. Torkelson, "Effective SNR estimation in OFDM system simulation," in *Proc. IEEE Global Telecommun. Conf. (Globecom'98)*, vol. 2, Nov. 1998, pp. 945–950.

[10] B. O'Hara and A. Petrick, *The IEEE* 802.11 *handbook: A designer's companion*. Standard Information Network IEEE Press, 1999.

[11] *Wireless LAN Medium Access Control (MAC) and Physical Layer (PHY) Specifications: High-Speed Physical Layer in 5GHz Band*, IEEE Std. 802.11a, Sep 1999.